Published in final edited form as:
Neuron. 2008 October 23; 60(2): 298–307. doi:10.1016/j.neuron.2008.08.028.

Dendritic NMDA receptors activate axonal calcium channels

Jason M. Christie[1] and **Craig E. Jahr**[1]

1*Vollum Institute, Oregon Health & Science University Portland, OR USA*

Summary

NMDA receptor (NMDAR) activation can alter synaptic strength by regulating transmitter release from a variety of neurons in the CNS. As NMDARs are permeable to Ca^{2+} and monovalent cations, they could alter release directly by increasing presynaptic Ca^{2+} or indirectly by axonal depolarization sufficient to activate voltage-sensitive Ca^{2+} channels (VSCCs). Using two-photon microscopy to measure Ca^{2+} excursions, we found that somatic depolarization or focal activation of dendritic NMDARs elicited small Ca^{2+} transients in axon varicosities of cerebellar stellate cell interneurons. These axonal transients resulted from Ca^{2+} entry through VSCCs that were opened by the electrotonic spread of the NMDAR-mediated depolarization elicited in the dendrites. In contrast, we were unable to detect direct activation of NMDARs on axons indicating an exclusive somatodendritic expression of functional NMDARs. In cerebellar stellate cells, dendritic NMDAR activation masquerades as a presynaptic phenomenon and may influence Ca^{2+}-dependent forms of presynaptic plasticity and release.

Introduction

NMDARs are found throughout the central nervous system and contribute to synaptic excitability and intracellular Ca^{2+} transients. NMDARs were once thought to be expressed exclusively in somatodendritic membranes, concentrated at the postsynaptic density of glutamatergic synapses (Fagg and Matus, 1984; Monaghan and Cotman, 1986). An emerging view suggests that NMDARs are also expressed in axons because NMDAR activation can alter spontaneous and action potential-evoked transmitter release (Berretta and Jones, 1996; Bardoni et al., 2004; Sjostrom et al., 2003; Corlew et al., 2007; Yang et al., 2006; Brasier and Feldman, 2008). Given the Ca^{2+}-dependence of neurotransmitter release and modulation (Zucker and Regehr, 2002), these results imply that there is a close spatial association of NMDARs and presynaptic release sites because of the limited intracellular diffusion of NMDAR-mediated Ca^{2+} entry (Mainen et al. 1999; Sabatini et al. 2002). However, results from dentate granule cells and cortical pyramidal cells indicate that subthreshold somatodendritic depolarizations can enhance axonal release by passively depolarizing axonal release sites (Alle and Geiger, 2006; Shu et al., 2006). It is possible, then, that potentiation of release by NMDARs is caused, at least in part, by somatodendritic NMDAR activation and passive propagation of the resulting depolarization to axonal release sites.

Stellate cells are a class of interneuron located in the molecular layer of cerebellar cortex (Palay and Chan-Palay, 1974). They express NMDARs in an atypical pattern in their dendrites

Address for Correspondence: Jason M. Christie, Vollum Institute, Oregon Health & Science University, 3181 SW Sam Jackson Park Road, Portland, OR 97239-3098, Phone: (503) 494-0759, Fax: (503) 494-6972, Email: christij@ohsu.edu.

in that they surround the postsynaptic density rather than reside within it (Clark and Cull-Candy, 2002). Several studies report that NMDARs are also expressed on the axons of stellate cells. In the absence of action potentials, bath application of NMDA increases the rate of spontaneous exocytotic release of GABA from stellate cells onto Purkinje cells (Glitsch and Marty, 1999; Duguid and Smart, 2004; Huang and Bordey, 2004; Glitsch, 2008) and elevates Ca^{2+} in their axons (Shin and Linden, 2005).However, direct detection of presynaptic NMDA receptors remains elusive (Clark and Cull-Candy, 2002) and the contribution of somatodendritic NMDARs to axonal Ca^{2+} elevation has not been determined.

In this study, we have investigated the distribution of NMDARs in stellate cells using two-photon laser-scanning microscopy and Ca^{2+} imaging. We find that NMDARs are expressed on dendrites but not on axons. However, Ca^{2+} transients are evoked in axons by activation of dendritic NMDARs either by exogenous agonists or synaptic stimulation. NMDAR-mediated Ca^{2+} transients in stellate cell axons result from VSCCs opened by passive spread of the dendritic NMDAR depolarization. Our results suggest that NMDAR depolarization-mediated Ca^{2+} transients in axons will have a profound influence on release.

Results

NMDAR-mediated Ca^{2+} transients in stellate cell dendrites and axons

To probe for NMDAR activity we imaged Ca^{2+} transients evoked by bath applied NMDA (10 μM) in the axons and dendrites of stellate cells in rat cerebellar slices (0 mM Mg^{2+}, 0.5 μM TTX). Cells were filled through the patch pipette with the red fluophore Alexa 594 (50 μM) to visualize cell morphology and the green calcium indicator Fluo-5F (200 μM) for measuring Ca^{2+} transients. After loading, dendrites and axons were easily resolved (Figure 1A). Axons were distinguished by a long, complex plexus of collaterals studded with varicosities whereas dendrites were short and not varicose (Palay and Chan-Palay, 1974). Images of dendrites during NMDA application revealed large increases in intracellular Ca^{2+} in current-clamped stellate cells (Figure 1B) consistent with the activation of Ca^{2+}–permeable NMDARs (MacDermott et al. 1986). Concurrent with the rise in Ca^{2+}, NMDA application also resulted in a significant depolarization (17.7 ± 0.6 mV, n= 28) of the stellate cell as recorded in the soma (Figure 1B). The large magnitude of the NMDAR-mediated response is attributable to the absence of extracellular Mg^{2+} that, when present, blocks NMDARs in a voltage-dependent manner (Mayer et al., 1984;Nowak et al. 1984). For example, with 1 mM extracellular Mg^{2+}, 30 μM NMDA, the concentration used in previous reports (Glitsch and Marty, 1999; Huang and Bordey,2004; Glitsch 2008), was required to generate a depolarization of similar size (22.4 ± 1.1 mV, n= 5). It is unlikely that Ca^{2+} influx through VSCCs contributed significantly to the NMDA-evoked Ca^{2+} transient recorded in the dendrite because direct depolarization by somatic current injection resulted in very little Ca^{2+} elevation (Figure 1B).

We then imaged the bead-like varicosities along axons for NMDAR-mediated Ca^{2+} influx (Shin and Linden, 2005) where the activation of axonal NMDARs is thought to increase the rate of spontaneous inhibitory neurotransmission (Glitsch and Marty,1999; Duguid and Smart, 2004; Huang and Bordey, 2004; Glitsch 2008). Axon varicosities are hot spots of action potential-evoked Ca^{2+} entry (Figure $1C_1$) indicative of clustered VSCC activity and therefore are presumed *en passant* sites of release (Palay and Chan-Palay, 1974; Llano et al., 1997; Forti et al., 2000). We found that bath application of NMDA (10 and 30 μM; 0 and 1 mM Mg^{2+}, respectively) also resulted in an elevation of Ca^{2+} in axon varicosities (Figure $1C_2$ and 1D, $\Delta G/R = 0.0219 \pm 0.0043$, n=30; $\Delta G/R = 0.0090 \pm 0.0005$, n= 5, 10 and 30 μM NMDA, respectively, p= 0.24).However, the Ca^{2+} rise in axons was much smaller than that recorded in dendrites ($p < 0.05$). In contrast to dendrites, matching the NMDA-induced depolarization by somatic current injection resulted in a Ca^{2+} elevation in the axon that was indistinguishable from the transient evoked by bath applied NMDA (n= 4, p= 0.64; Figure $1C_2$). This suggests

that NMDAR-dependent Ca^{2+} elevation in axon varicosities is controlled by membrane potential and VSCCs rather than direct Ca^{2+} influx through NMDA receptors.

If axonal NMDARs mediate the depolarization underlying Ca^{2+} accumulation in axon varicosities, then bath NMDA-evoked Ca^{2+} transients should be observed throughout the axonal arbor. However, we found that NMDA-evoked Ca^{2+} transients in proximal axon varicosities were often much larger than those evoked in distal varicosities (Figure 1D). Nonlinear regression analysis revealed an inverse correlation (r^2= 0.98) between the amplitude of the Ca^{2+} increase in axon varicosities and distance from the soma. A monoexponential fit of binned data (50 μm bins) yielded a decay length constant of 212 μm. We therefore propose that NMDA-evoked Ca^{2+} elevation in axons results from an NMDAR depolarization originating in the somatodendritic compartment that passively propagates into the axon.

Dendritic NMDAR potentials and axonal Ca^{2+} entry

To determine if depolarization resulting from selective activation of dendritic NMDARs is sufficient to control axonal Ca^{2+} entry without the concomitant activation of axonal NMDARs, we used iontophoresis of the NMDAR agonist *L*-aspartate to locally activate NMDARs on stellate cell dendrites (Figure $2A_1$) in the presence of TTX (0.5 μM). In current-clamped cells, dendritic iontophoresis of *L*-aspartate (−50 to −200 nA; 10–50 msec) elicited brief NMDAR-mediated potentials (29.8 ± 1.7 mV, n=13; Figure $2A_2$) that resembled EPSPs (see Figure $7A_2$) and evoked Ca^{2+} transients in dendrites near the iontophoretic pipette (Figure 2B and 2C). The NMDAR antagonist (*R*)-CPP (20 μM) blocked the Ca^{2+} transient evoked by iontophoresis (ΔG/R 5.9 ± 4.3% of control, n= 7;Figure 2C) indicating that the Ca^{2+} transient was NMDAR-mediated. We found that dendritic *L*-aspartate iontophoresis also evoked Ca^{2+} transients in axon varicosities (Figure 2D). These transients were much smaller in amplitude than action potential-evoked Ca^{2+} transients in axon varicosities or the Ca^{2+} transients evoked by iontophoresis recorded in the dendrite (Figure 2D and 2E).

We confirmed that the axonal Ca^{2+} transient depended on the NMDAR-mediated depolarization originating in the dendrite by voltage-clamping the soma. This manipulation prevents the passive propagation of dendritic depolarization into the axon and eliminated iontophoresis-evoked Ca^{2+} entry in axon varicosities (Figure 2F and 2H). This observation is reminiscent of experiments in dentate granule cells and cortical pyramidal cells showing that subthreshold depolarizations originating in the somatodendritic domain can passively propagate into axons (Alle and Geiger, 2006; Shu et al., 2006). Similarly, somatic voltage-clamp dramatically reduced the bath NMDA-evoked Ca^{2+} transient recorded in axon varicosities (ΔG/R 25.3 ± 7.5% of current-clamp,n= 3; $p< 0.05$) suggesting a similar pathway of Ca^{2+} entry. The Ca^{2+} component remaining in voltage-clamp probably reflects diffusion of Ca^{2+} from the dendrite into the axon during prolonged bath application of NMDA. In contrast, somatic voltage-clamp did not alter the dendritic Ca^{2+} transient evoked by *L*-aspartate iontophoresis (Figure 2G and 2H) indicating that the dendritic signal is the result of Ca^{2+} influx through local NMDARs.

Cable theory predicts that nonregenerative potentials will passively decay along lengths of dendrite and axon (Rall 1969). Therefore, distance-dependent shaping of depolarizing potentials that control Ca^{2+} entry in axon varicosities should be reflected in the amplitude and shape of the evoked Ca^{2+} transient. As with bath applications of NMDA, the amplitudes of *L*-aspartate iontophoresis-evoked Ca^{2+} transients were largest in proximal varicosities and decreased with distance from the soma (ΔG/R= 0.0154 ±0.0038, n=17; and ΔG/R= 0.0019 ± 0.0013, n=7; <150 μm and ≥150μm respectively; $p< 0.05$) (Figure 3A–3C). In addition, there was a trend for faster Ca^{2+} transients in proximal varicosities, however, small amplitude transients, especially in distal axonal segments, prevented accurate fitting of rise times for all

data points (Figure 3B and 3D). Together, these results indicate that NMDAR-mediated potentials originating in the dendrite can control Ca^{2+} entry in axon varicosities.

Dendritic NMDAR-mediated depolarizations open axonal VSCCs

It is likely that NMDAR-mediated Ca^{2+} entry in axon varicosities occurs through VSCCs because this effect depends on membrane potential and VSCCs are enriched in stellate cell presynaptic specializations (Llano et al., 1997; Forti et al., 2000). Consistent with this notion, a cocktail of VSCC blockers (ω-conotoxin MVIIC 1 μM, SNX 0.3 μM,ω-agatoxin IVA 0.2 μM, nimodipine 20 μM and mibefradil 10 μM) greatly reduced the Ca^{2+} transient evoked in axon varicosities by dendritic-targeted iontophoresis of *L*-aspartate (Figure 4A and 4D). The unblocked component likely reflects toxin-resistant Ca^{2+} channels (Tottene et al. 2000; Metz et al. 2005; Li et al. 2007) given that action potential-evoked Ca^{2+} transients in axon varicosities were blocked to a similar extent (Figure 4B and 4D). In contrast, iontophoresis-evoked Ca^{2+} transients in dendrites were unaltered by VSCC blockers (Figure 4C and 4D) indicating that most Ca^{2+} entry in this compartment was directly through NMDARs.

NMDARs are not expressed on axons

Our results indicate that NMDAR-mediated Ca^{2+} entry in axon varicosities does not result from direct influx through axonal NMDARs but rather that NMDAR-mediated depolarization, most likely from dendritic receptors, results in Ca^{2+} influx through VSCCs. If NMDARs were expressed on the axon then axonal *L*-aspartate iontophoresis would increase axonal Ca^{2+} directly through NMDARs. However, in voltage-clamped cells, *L*-aspartate iontophoresis failed to evoke Ca^{2+} transients in axon varicosities when focally applied near the axon (ΔG/R= 0.0004 ± 0.0002, n=33; Figure 5A and 5B). Iontophoresis of *L*-aspartate onto dendrites prior to and following axonal application elicited large Ca^{2+} transients in the dendrites (Figure 5A and 5B) and inward currents (−24.3 ± 3.8 pA, n= 10) in somatic electrical recordings confirming the reliability of iontophoresis within single cell experiments. No current was detected when *L*-aspartate was applied near the axon (−0.2 ± 0.1 pA, n= 24) similar to the results of Clark and Cull-Candy (2002). Fluorescence measurements obtained from axon varicosities following direct iontophoretic stimulation were unchanged by (*R*)-CPP (20 μM) (ΔG/R 114.8 ± 29.3% of control, n= 15) confirming that axon varicosities lack functional NMDARs. It is unlikely that low-density NMDAR expression mediated Ca^{2+} transients that were below detection threshold given that two-photon fluorescence imaging has the sensitivity to detect Ca^{2+} entry through single channels (Sabatini and Svoboda, 2000; Nimchinsky et al. 2004; see Experimental Procedures).

To examine a larger axonal area than afforded by line scans, frame scans were used to image small regions of axons (Figure 6A–D). As with line scans, we were unable to detect elevations of Ca^{2+} in axonal varicosities following iontophoretic application of *L*-aspartate near the axon of interest (ΔG/R= 0.0006 ± 0.0005, n= 14). Action potential-evoked Ca^{2+} transients confirmed that the selected sites were hot spots of Ca^{2+} entry (Figure 6C). In addition, NMDAR-dependent Ca^{2+} transients were not detected in axon segments between varicosities (ΔG/R= 0.0004 ± 0.0006, n= 9; Figure 6C and 6D). These results suggest that the entire axonal arbor is devoid of functional NMDARs. Therefore, dendritic NMDARs must provide the sole source of depolarization responsible for NMDAR-mediated Ca^{2+} entry in axon varicosities.

NMDAR-mediated EPSPs evoke Ca^{2+} entry in axon varicosities

We next determined whether synaptic stimulation could produce NMDAR-mediated Ca^{2+} transients in axon varicosities similar to those evoked by bath applied NMDA and dendritic *L*-aspartate iontophoresis. Subthreshold NMDAR-mediated EPSPs (17.6 ± 0.7 mV, n= 23) were evoked in current-clamped cells by extracellular stimulation (50 Hz, 80–140 ms) of parallel fibers (PFs) near the dendritic arbor (Figure $7A_1$ and $7A_2$). PF stimulation elicited large

Ca^{2+} transients localized to dendrites near the stimulating pipette (ΔG/R= 0.1994 ± 0.0338, n=8; Figure 7B; Figure S1A). The spatial extent of Ca^{2+} accumulation was larger than expected from single synapses (Soler-Llavian and Sabatini,2006) owing to the stimulation of multiple PFs, the extrasynaptic localization of NMDARs and glutamate spillover (Carter and Regehr, 2000; Clark and Cull-Candy, 2002). Ca^{2+} transients were also evoked in axon varicosities by dendrite-targeted PF stimulation (Figure 7B). These Ca^{2+} transients were smaller than those evoked by dendritic iontophoresis (ΔG/R= 0.0110 ± 0.0029, n=24; and ΔG/R= 0.0027 ± 0.0006, n=37, iontophoretic and synaptic stimulation, respectively; $p< 0.05$) most likely because iontophoretically evoked potentials were larger in amplitude ($p< 0.05$). (*R*)-CPP (20 μM) blocked PF-evoked Ca^{2+} transients in both dendrites and axon varicosities (ΔG/R 2.8 ± 1.9% of control, n= 3; and 1.0 ± 6.3% of control, n= 5; dendrites and axon varicosities, respectively) confirming that the transients were NMDAR-mediated (Figure S1B and S1C). As with iontophoretic stimulation of dendritic NMDARs, somatic voltage clamp greatly reduced the PF-evoked Ca^{2+} transient recorded in axon varicosities but not in the dendrite (ΔG/R 13.8 ± 9.0%, n= 7; and 95.7 ± 1.8% of control amplitude, n= 5, axon varicosity and dendrite, respectively; $p< 0.05$; Figure $7C_1$ and $7C_2$) indicating that the passive propagation of somatodendritic depolarization evoked axonal Ca^{2+} entry.

Positioning the stimulating pipette adjacent to axon varicosities so that local PFs were excited failed to elevate Ca^{2+} (Figure 7D and 7E) again suggesting that there are no functional axonal NMDARs. That axonal Ca^{2+} transients evoked by dendritic PF stimulation rely on passive propagation of somatic depolarizations is further supported by the dependence of their amplitudes on the distance from the soma (Figure S2). Nonlinear regression analysis revealed that the amplitude of these axonal Ca^{2+} transients was inversely correlated ($r^2= 0.89$) with distance from the soma with a monoexponential fit (50 μm bins) yielding a decay length constant of 60 μm (Figure S2C). In contrast, the amplitude of action potential-evoked Ca^{2+} transients in axon varicosities varied irrespective of distance ($r^2= 0.03$).

Discussion

Axonal expression of NMDARs has been reported in many regions of the CNS (Berretta and Jones, 1996; Bardoni et al., 2004; Sjostrom et al., 2003; Corlew et al., 2007; Yang et al., 2006; Brasier and Feldman, 2008) including interneurons in the cerebellar cortex (Glitsch and Marty, 1999; Duguid and Smart, 2004; Huang and Bordey, 2004). However, we find that stellate cell axons are devoid of functional NMDARs. This result does not imply that NMDARs are without influence in the axon. NMDAR-mediated depolarizations originating in the dendrite passively propagated into the axon and opened VSCCs in varicosities where these channels are concentrated. This axonal Ca^{2+} transient is the likely basis for the increase in the strength and frequency of evoked and spontaneous release that have been reported previously (Glitsch and Marty, 1999; Duguid and Smart, 2004; Huang and Bordey, 2004).

Localization of NMDARs

Stellate cell dendrites express both AMPA and NMDA-type glutamate receptors. Whereas unitary PF responses are mediated entirely by AMPARs, NMDARs are recruited only under conditions of dense PF activity suggesting that they are located perisynaptically (Carter and Regehr, 2000; Clark and Cull-Candy, 2002). NMDAR immunoreactivity in the molecular layer of cerebellar tissue is consistent with dendriticand axonal expression in interneurons (Petralia et al., 1994). In cultured stellate cells,axon varicosities are immunolabeled with antibodies raised against NR1 and NR2 subunits (Duguid and Smart, 2004) and patches excised from axon terminals have functional NMDAR channels (Fiszman et al., 2005). However, despite large NMDAR-mediated Ca^{2+} influx in dendrites, our search failed to detect functional NMDARs in axons. In addition, preliminary evidence from basket cells suggests that the axons

of this cell type are also devoid of functional NMDARs (unpublished observations), indicating a commonality between the major inhibitory interneurons in the cerebellar molecular layer.

Our method of locating NMDARs depends on the generation of Ca^{2+} influx. Ca^{2+} permeability is diminished when heteromeric NMDA channels incorporate NR3 subunits (Matsuda et al., 2002; Sasaki et al., 2002). It is unlikely that NR3 expression in stellate cells obscured observation of NMDAR-dependent Ca^{2+} entry given that the cerebellum lacks NR3A and NR3B subunits at postnatal day (PND)> 14 (Ciabarra et al., 1995; Sucher et al., 1995; Nishi et al., 2001; Fukaya et al., 2005; but see Wee et al. 2008). If axonal NR3 subunit-containing receptors were activated, then the resulting local depolarization should cause a VSCC-mediated Ca^{2+} transient. However, axonal Ca^{2+} transients were not evoked by local stimulation, but rather, only by manipulations that depolarized the somatodendritic compartment. Therefore, at the very least, NMDAR-dependent dendritic depolarization must be a greater influence on axonal Ca^{2+} entry.

Passive Propagation of Dendritic Depolarization

Excitatory potentials from the somatodendritic compartment passively propagate into the axonal arbor of neurons in the hippocampus and neocortex (Alle and Geiger, 2006; Shu et al., 2006), as they do in frog sciatic nerve (Hodgkin, 1937). Although direct electrical measurements did not reveal VSCC openings in dentate granule cell boutons (Alle and Geiger, 2006), an experimentally derived model suggests that subthreshold waveforms should activate a small population of VSCCs (Li et al., 2007). This discrepancy could result from the difficulty in recording VSCC activity mediated by small depolarizations (Awartramani et al., 2005). Our results indicate that NMDAR-mediated potentials passively propagate from the stellate cell dendrite into the axon and that the resulting voltage waveform is sufficient to open VSCCs in varicosities. Passively propagated NMDAR currents originating in the dendrite were also detected in direct electrical recordings from proximal axon varicosities of cerebellar interneurons in culture (Fiszman et al., 2005).

NMDAR depolarization-evoked Ca^{2+} transients in stellate cell axons were largest in proximal axon varicosities and diminished in size with distance from the soma consistent with passive propagation (Rall 1969). The length constant measured for PF-evoked transients was less than 100 μm, a relatively short distance when compared to the length constants of electrotonic propagation in pyramidal and dentate granule cell axons ($\tau \approx 400$ μm; Alle and Gieger, 2006; Shu et al., 2006). In our measurements, VSCC-mediated Ca^{2+} influx is secondary to the underlying depolarization and most likely not linearly related to depolarization. Likewise, somatic voltage control of action potential-evoked Ca^{2+} transients in mossy fiber boutons decayed with a length constant of $\tau < 200$ μm (Scott and Rusakov, 2006). The effectiveness of this transfer is determined by many factors including the electrotonic structure of the cell (Rall, 1969), number and type of Ca^{2+} channels (Li et al., 2007), and the size and time course of the underlying potential (Shu et al., 2006). For example, the length constant of bath NMDA-evoked Ca^{2+} entry extended beyond 200 μm, probably owing to the prolonged duration of the underlying depolarization. The axonal arbors of stellate cells are relatively compact with the most distal collaterals rarely extending more than 400 μm from the soma (Palay and Chan-Palay, 1974). Therefore, the length constant derived for bath NMDA and PF-evoked Ca^{2+} transients suggests that varicosities throughout a large portion of the stellate cell axonal arbor are influenced by passively propagated depolarizations. In neurons with extensive axon arbors, such as dentate granule cells, length constants of similar distance are unlikely to influence much of the axon (Scott et al., 2008).

Ca^{2+} diffusion is tightly regulated in small neuronal structures by endogenous, low-mobility buffers, pumps and the morphological specialization (Sabatini et al. 2002; Goldberg et al., 2003; Soler-Llavian and Sabatini, 2006; Brenowitz and Regehr, 2007). In CA1 pyramidal cell

spines, for example, NMDAR-mediated Ca^{2+} entry is so well compartmentalized that it is insufficient to activate SK channels expressed on the same spines (Bloodgood and Sabatini, 2007). Similarly, Ca^{2+} influx through NMDARs located at olfactory bulb dendrodendritic synapses does not normally trigger release of nearby GABA-filled vesicles (Isaacson, 2001; but see Chen et al. 2000; Halabisky et al. 2000). The effects of Ca^{2+} influx through NMDARs, then, are usually restricted to sub-micron domains. The coupling of VSCC activity to passively propagated NMDAR-mediated potentials provides a mechanism to extend the spatial extent of NMDAR Ca^{2+} signaling beyond simple diffusion.

Functional Implications

Neurotransmission is both triggered and modulated by Ca^{2+} signals in presynaptic elements. Although high concentration Ca^{2+} transients are required to trigger exocytosis,low concentrations precondition vesicles for release via vesicle recruitment, priming and sensitization (Zucker and Regehr, 2002). Short-term elevation of $Ca2^{+}$ occurring, for example, following an action potential leads to facilitation of synaptic transmission to subsequent action potentials (Zucker and Regehr, 2002). Axonal Ca^{2+} may also be elevated directly by ligand-gated channels that are expressed on the bouton that either depolarize the bouton, are permeable to Ca^{2+}, or both (MacDermott et al., 1999; Engelman and MacDermott, 2004). Our results indicate that dendritic ligand-gated channels can elevate Ca^{2+} in stellate cell axon varicosities by electrotonic propagation thereby providing an alternative method for elevating Ca^{2+} at presynaptic sites of release.

Although we did not determine the relationship between somatodendritic depolarization-mediated Ca^{2+} entry and release, a facilitatory role is clearly implied from previous investigations in the cerebellum (Glitsch and Marty, 1999; Duguid and Smart,2004; Huang and Bordey, 2004). Recent studies have shown that in neocortical pyramidal cells and dentate granule cells of the hippocampus, passive propagation of somatodendritic depolarization into boutons facilitates release (Alle and Geiger, 2006; Shu et al., 2006). Ca^{2+} elevation was found to be only partly responsible (Alle and Geiger, 2006) suggesting that other mechanisms also contribute to this facilitation (Shu et al., 2006; Kole et al., 2007; Scott et al., 2008). In the calyx of Held, slight depolarization of the presynaptic element by direct current injection results in a small increase in Ca^{2+} and a significant enhancement of synaptic transmission (Awartramani et al., 2005), demonstrating the critical relationship between residual Ca^{2+} and the likelihood of vesicle release. Given the large charge transfer mediated by NMDAR synaptic conductances and the long time constant of the compact stellate cells, dendritic depolarization-mediated Ca^{2+} entry could alter the axonal release probability for significant periods.

Activation of presynaptic VSCCs by dendritic depolarization may be a general feature of neurotransmitter release plasticity. Our measurements of dendritic depolarization-evoked Ca^{2+} transients in axon varicosities were limited to NMDAR-mediated activity and current injection through the patch pipette. It is likely that other ypes of ligand-gated ion channels expressed on the dendrite also control axonal VSCC activation. AMPAR activation elicited by synaptic stimulation or exogenously applied agonists alters the strength and frequency of action potential-evoked and spontaneous release in cerebellar interneurons (Bureau and Mulle, 1998; Satake et al., 2000; Satake et al., 2004; Rusakov et al. 2005; and Liu 2007). Although these effects were ascribed to receptors expressed on axons, VSCCs are at least partly responsible for the observed affect (Bureau and Mulle, 1998). It is clear that multiple mechanisms can alter presynaptic release probability including residual Ca^{2+} from previous action potentials, ligand-gated receptors expressed on axons, and subthreshold activation of axonal VSCCs either by direct axonal depolarization or passive propagation from dendritic sites.

Experimental Procedures

Slice Preparation and Electrophysiology

Following anesthesia, cerebellar vermi from Sprague Dawley rats (PND 15–20) were isolated and cut parasagittally (250–300 μm) on a vibroslicer (Leica Instruments, Nussloch, Germany) in an ice-cold solution containing (in mM) 87 NaCl, 25 $NaHO_3$, 2.5 KCl, 1.25 NaH_2PO_4, 7 $MgCl_2$, 0.5 $CaCl_2$, 10 glucose, and 75 sucrose. Slices were then transferred to a chamber containing artificial cerebrospinal solution (ACSF) containing (in mM) 119 NaCl, 26.2 $NaHO_3$, 2.5 KCl, 1 NaH_2PO_4, 1.3 $MgCl_2$, 2 $CaCl_2$, 11 glucose and incubated at 34°C for 30 min. Thereafter, slices were maintained at 22–25°C. During recordings, slices were superfused with ACSF (22–25°C) altered to facilitate the detection of NMDAR-mediated calcium transients (0 mM $MgCl_2$, 3 mM $CaCl_2$). NBQX (20 μM) and picrotoxin (100 μM) were added to block AMPA and $GABA_A$ receptors, respectively, *D*-serine (10 μM) was added to saturate the NMDAR coagonist-binding site, and cyclopiazonic acid (CPA; 20 μM) was used to deplete internal Ca^{2+} stores. All solutions were bubbled with 95% O_2- 5% CO_2. Animal handling and procedures were performed in accordance with Oregon Health and Science University Institutional Animal Care and Use Committee protocols.

Whole-cell recordings were obtained from stellate cells identified with gradient contrast infrared optics (Dodt et al., 2002) and two-photon fluorescence microscopy based on their location in the molecular layer and distinct morphology (Palay and Chan-Palay, 1974). Pipettes with resistances of 3–4 MΩ were used for patching and contained a solution of (in mM) 142 K-gluconate, 2 KCl, 10 HEPES, 4 $MgCl_2$, 4 NaATP, 0.5 NaGTP, 0.05 Alexa 594 and 0.2 Fluo-5F (Molecular Probes, Eugene, OR). Electrophysiological potentials and currents were recorded with a Multiclamp 700B amplifier (Molecular Devices, Union City, CA). Electrode series resistance was compensated by bridge balance. The analog signals were filtered at 3–10 kHz and digitized at 10–20 kHz. Data were collected using custom software (J.S. Diamond) written in IgorPro (Wavemetrics, Lake Oswego, OR). Action potentials were evoked by current injection (100–175 pA; 5–10 msec) through the patch pipette. Parallel fibers were stimulated with a pipette filled with ACSF (10–100 V, 30–100 μsec). Iontophoretic pipettes (impedance >100 MΩ) were filled with a 1M solution of *L*-aspartate (pH 7.0).Pipettes were placed near (5–20 μm) the cellular process of interest. A retention current of ≈−1 nA was applied to prevent passive leakage of *L*-aspartate while a pulse of 100–200 nA (10–50 msec) was used for ejection. TTX (0.5 μM) was bath applied prior to iontophoretic stimulation in order to prevent the initiation of action potentials.

Pharmacological agents including NBQX, CPA, TTX, and NMDA were obtained from Tocris Cookson (Ellisville, MO). Picrotoxin, nimodipine and mibefradil were from Sigma (St. Louis, MO). Peptides including ω-conotoxin MVIIC, SNX, and ω-agatoxin IVA were purchased from Peptides International (Louisville, KY). CytoC or BSA (Sigma, St. Louis, MO) was added (0.25 mg per ml) to solutions containing peptides to prevent surface adsorption in the perfusion system.

Two-photon Imaging

Fluorescence was monitored with a lab-built two-photon laser-scanning microscope using an Olympus (Melville, NY) upright microscope and objective (60X,0.9 NA) and a Ti:sapphire laser (Coherent, Santa Clara, CA) tuned to 810 nm. Green and red fluorescence was simultaneously collected by photomultiplier tubes (H8224, Hamamatsu, Hamamatsu City, Japan) in both epi- and transfluorescence pathways using a 565 nm dichroic and 525/50 and 620/60 bandpass filters (Chroma, Battleboro, VT). Images were acquired using ScanImage software (Pologruto et al., 2004). Lines scans were obtained at 500 Hz while sequential frame scanning occurred at 7.8 Hz. Fluorescence changes were quantified as increases in green

fluorescence normalized to red fluorescence (ΔG/R) (Sabatini et al. 2002). Peak amplitude measurements of evoked Ca^{2+} transients (except for action potentials) reflect the average ΔG/R of a 250 msec epoch centered on the peak. For most axonal line scan measurements, alternating trials in which no stimulation occurred were used to subtract background fluorescence levels.

Sensitivity of fluorescence detection

To estimate the Ca^{2+} signal-detection sensitivity of our microscope, we examined VSCC-mediated Ca^{2+} transients evoked by somatic action potentials in spicules (Figure S3A), the spine-like protrusions located on stellate cell dendrites (Palay and Chan-Palay, 1974). We observed extensive variability in the peak response of evoked transients in individual spicules whereas evoked transients in the attached parent dendrite varied less (≥50 trials) (Figure S3B). As with action-potential evoked Ca^{2+} transients in spines of CA1 pyramidal cells (Sabatini and Svoboda, 2000), we were able to detect obvious failures in several spicules. These failures did not result from action potential propagation failure because Ca^{2+} transients were detected in the parent dendrite in the same trial and the amplitude of the evoked dendritic Ca^{2+} transient was independent of the Ca^{2+} transient in the spicule (Figure $S3C_1$ and $S3C_2$). The failure rate in spicules ranged from 0.05–0.28 (average 0.16 ± 0.05; n= 4). Given the probabilistic nature of VSCC opening it is likely that Ca^{2+} transients mediated by single channels were also recorded in some trials (Sabatini and Svoboda, 2000).

Although the Ca^{2+} permeability of NMDA and VSCCs is not dissimilar (Hille 2001), NMDA channels produce a much greater influx of total Ca^{2+} following activation due to their long open time (NMDAR open times ~100 msec, Lester et al. 1990; action potential-mediated open time for VSCCs <1 msec, Bischofberger et al. 2002). In estimates from CA1 pyramidal cell spines where single NMDA channel-mediated Ca^{2+} transients have been measured (Nimchinsky et al. 2004), Ca^{2+} influx through NMDARs activated by synaptic transmission is at least ten-fold greater than VSCC-mediated Ca^{2+} influx evoked by an action potential (Sabatini and Svoboda, 2000; Sabatini et al., 2002). Therefore, if we can detect Ca^{2+} influx mediated by single VSCCs in dendrites, we should be able to detect Ca^{2+} influx through single NMDARs in dendrites or axons.

Data Analysis

Excel (Microsoft) and InStat (GraphPad Software) were used for statistical analysis. ANOVA (Bonferroni post hoc procedures) and t-tests were used as appropriate. A value of $p < 0.05$ was considered significant. Reported values are mean ± SEM. In figures asterisks denote statistical significance.

Supplementary Material

Refer to Web version on PubMed Central for supplementary material.

Acknowledgments

We thank Kevin Bender, Vanessa Bender, Melissa Herman, Richard Piet and Jason Pugh for their helpful discussions and comments on the manuscript. This work was supported by National Institute of Health Grant NS40056 (CEJ).

References

Alle H, Geiger JRP. Combined analog and action potential coding in hippocampal mossy fibers. Science 2006;311:1290–1293. [PubMed: 16513983]

Awatramani GB, Price GD, Trussell LO. Modulation of transmitter release by presynaptic resting potential and background calcium levels. Neuron 2005;48:109–121. [PubMed: 16202712]

Bardoni R, Torsney C, Tong CK, Prandini M, MacDermott AB. Presynaptic NMDA receptors modulate glutamate release from primary sensory neurons in rat spinal cord dorsal horn. J. Neurosci 2004;24:2774–2781. [PubMed: 15028770]

Berretta N, Jones RS. Tonic facilitation of glutamate release by presynaptic N-methl-D-aspartate autoreceptors in entorhinal cortex. Neuroscience 1996;75:339–344. [PubMed: 8931000]

Bischofberger J, Geiger JR, Jonas P. Timing and efficacy of Ca^{2+} channel activation in hippocampal mossy fiber boutons. J. Neurosci 2002;22:10593–105602. [PubMed: 12486151]

Bloodgood BL, Sabatini BL. Nonlinear regulation of unitary synaptic signals by $CaV_{2.3}$ voltage-sensitive calcium channels located in dendritic spines. Neuron 2007;53:249–260. [PubMed: 17224406]

Brasier DJ, Feldman DE. Synapse-specific expression of functional presynaptic NMDA receptors in rat somatosensory cortex. J. Neurosci 2008;28:2199–2211. [PubMed: 18305253]

Brenowitz SD, Regehr WG. Reliability and heterogeneity of calcium signaling at single presynaptic boutons of cerebellar granule cells. J. Neurosci 2007;27:7888–7898. [PubMed: 17652580]

Bureau I, Mulle C. Potentiation of GABAergic synaptic transmission by AMPA receptors in mouse cerebellar stellate cells: changes during development. J. Physiol 1998;509:817–831. [PubMed: 9596802]

Carter AG, Regehr WG. Prolonged synaptic currents and glutamate at the parallel fiber to stellate cell synapse. J. Neurosci 2000;20:4423–4434. [PubMed: 10844011]

Ciabarra AM, Sullivan JM, Gahn LG, Pecht G, Heinemann S, Sevarino KA. Cloning and characterization of χ-1; a developmentally regulated member of a novel class of the ionotropic glutamate receptor family. J. Neurosci 1995;15:6498–6508. [PubMed: 7472412]

Chen WR, Xiong W, Shepherd GM. Analysis of relations between NMDA receptors and GABA release at olfactory bulb reciprocal synapses. Neuron 2000;25:625–633. [PubMed: 10774730]

Clark BA, Cull-Candy SG. Activity-dependent recruitment of extrasynaptic NMDA receptor activation at an AMPA receptor-only synapse. J. Neurosci 2002;22:4428–4436. [PubMed: 12040050]

Corlew R, Wang Y, Ghermazien H, Erisir A, Philpot BD. Developmental switch in the contribution of presynaptic and postsynaptic NMDA receptors to long-term depression. J. Neurosci 2007;27:9835–9845. [PubMed: 17855598]

Duguid IC, Smart TG. Retrograde activation of presynaptic NMDA receptors enhance GABA release at cerebellar interneuron-Purkinje cell synapses. Nat. Neurosci 2004;7:525–533. [PubMed: 15097992]

Dodt HU, Eder M, Schierloh A, Zieglgansberger W. Infrared-guided laser stimulation of neurons in brain slices. Sci STKE 2002;2002PL2

Engelman HS, MacDermott AB. Presynaptic ionotropic receptors and control of transmitter release. Nat. Rev. Neurosci 2004;5:135–145. [PubMed: 14735116]

Fagg GE, Matus A. Selective association of N-methyl aspartate and quisqualate types of L-glutamate receptor with brain postsynaptic densities. Proc. Natl. Acad. Sci. USA 1984;81:6876–6880. [PubMed: 6149551]

Fiszman ML, Barberis A, Lu C, Fu Z, Erdelyi F, Szabo G, Vicini S. NMDA receptors increase the size of GABAergic terminals and enhance GABA release. J. Neurosci 2005;25:2024–2031. [PubMed: 15728842]

Forti L, Pouzat C, Llano I. Action potential-evoked Ca^{2+} signals and calcium channels in the axons of developing cerebellar interneurons. J. Physiol 2000;527:33–48. [PubMed: 10944168]

Fukaya M, Hayashi Y, Watanabe M. NR2 to NR3B subunit switchover of NMDA receptors in early postnatal motoneurons. Eur. J. Neurosci 2005;21:1432–1436. [PubMed: 15813953]

Glitsch M, Marty A. Presynaptic effects of NMDA in cerebellar Purkinje cells and interneurons. J. Neurosci 1999;19:511–519. [PubMed: 9880571]

Glitsch MD. Calcium influx through *n*-methy-d-aspartate receptors triggers GABA release at interneuron-Purkinje cell synapses in rat cerebellum. Neurosci 2008;151:403–409.

Goldberg JH, Tamas G, Aronov D, Yuste R. Calcium microdomains in aspiny dendrites. Neuron 2003;40:807–821. [PubMed: 14622584]

Halabisky B, Friedman D, Radojicic M, Strowbridge BW. Calcium influx through NMDA receptors directly evokes GABA release in olfactory bulb granule cells. J. Neurosci 2000;20:5124–5134. [PubMed: 10864969]

Hille, B. Sunderland, MA: Sinauer Associates; 2001. Ion Channels of Excitable Membranes.

Hodgkin AL. Evidence for electrical transmission in nerve. Part 1. J. Physiol 1937;90:183–210. [PubMed: 16994885]

Huang H, Bordey A. Glial glutamate transporters limit spillover activation of presynaptic NMDA receptors and influence synaptic inhibition in Purkinje neurons. J. Neurosci 2004;24:5659–5669. [PubMed: 15215288]

Isaacson JS. Mechanisms governing dendritic gamma-aminobutyric acid (GABA) release in the rat olfactory bulb. Proc. Natl. Acad. Sci. USA 2001;98:337–342. [PubMed: 11120892]

Kole MHP, Letzkus JJ, Stuart GJ. Axon initial segment Kv1 channels control action potential waveform and synaptic efficacy. Neuron 2007;55:633–647. [PubMed: 17698015]

Lester RA, Clements JD, Westbrook GL, Jahr CE. Channel kinetics determine the time course of NMDA receptor-mediated synaptic currents. Nature 1990;346:565–570. [PubMed: 1974037]

Li L, Bischofberger J, Jonas P. Differential gating and recruitment of P/Q-, N-, and R-type Ca^{2+} channels in hippocampal mossy fiber boutons. J. Neurocsi 2007;27:13420–13429.

Liu SJ. Biphasic modulation of GABA release from stellate cells by glutamatergic receptor subtypes. J. Neurophysiol 2007;98:550–556. [PubMed: 17537903]

Llano I, Tan YP, Caputo C. Spatial heterogeneity of intracellular Ca^{2+} siganls in axons of basket cells from the rat cerebellar slices. J. Physiol 1997;502:509–519. [PubMed: 9279804]

MacDermott AB, Mayer ML, Westbrook GL, Smith SJ, Barker JL. NMDA-receptor activation increases cytoplasmic calcium concentration in cultured spinal cord neurones. Nature 1986;321:519–522. [PubMed: 3012362]

MacDermott AB, Role LW, Siegelbaum SA. Presynaptic ionotropic receptors and the control of transmitter release. Ann. Rev. Neurosci 1999;22:443–485. [PubMed: 10202545]

Mainen ZF, Malinow R, Svoboda K. Synaptic calcium transients in single spines indicate that NMDA receptors are not saturated. Nature 1999;399:151–155. [PubMed: 10335844]

Matsuda K, Kamiya Y, Matsuda S, Yuzaki M. Cloning and characterization of a novel NMDA receptor subunit NR3B: a dominant subunit that reduces calcium permeability. Brain Res. Mol. Brain Res 2002;100:43–52. [PubMed: 12008020]

Mayer ML, Westbrook GL, Guthrie PB. Voltage-dependent block by Mg^{2+} of NMDA responses in spinal cord neurones. Nature 1984;309:261–263. [PubMed: 6325946]

Metz AE, Jarsky T, Martina M, Spruston N. R-type calcium channels contribute to afterdepolarization and bursting in hippocampal CA1 pyramidal neurons. J. Neurosci 2005;25:5763–5773. [PubMed: 15958743]

Monaghan DT, Cotman CW. Identification and properties of N-methyl-D-aspartate receptors in rat brain synaptic plasma membranes. Proc. Natl. Acad. Sci. USA 1986;83:7532–7536. [PubMed: 3020547]

Nimchinsky EA, Yasuda R, Oertner TG, Svoboda K. The number of glutamate receptors opened by synaptic stimulation in single hippocampal spines. J. Neurosci 2004;24:2054–2064. [PubMed: 14985448]

Nishi M, Hinds H, Lu HP, Kawata M, Hayashi Y. Motoneuron-specific expression of NR3B, a novel NMDA-type glutamate receptor subunit that works in a dominant-negative manner. J. Neurosci 2001;21RC185

Nowak L, Bregestovski P, Ascher P. Magnesium gates glutamate-activated channels in mouse central neurons. Nature 1984;307:462–465. [PubMed: 6320006]

Palay, SL.; Chan-Palay, V. Cerebellar cortex: cytology and organization. New York: Springer-Verlag; 1974.

Petralia RS, Wang YX, Wenthold RJ. The NMDA receptor subunits NR2A and NR2B show histological and ultrastructural localization patterns similar to those of NR1. J. Neurosci 1994;14:6102–6120. [PubMed: 7931566]

Pologruto TA, Sabatini BL, Svoboda BL. ScanImage: flexible software for operating laser scanning microscopes. Biomed. Eng. Online 2003;2:13. [PubMed: 12801419]

Rall W. Time constants and electrotonic length of membrane cylinders and neurons. Biophys. J 1969;9:1483–1508. [PubMed: 5352228]

Rusakov DA, Saitow F, Lehre KP, Konishi S. Modulation of presynaptic Ca^{2+} entry by AMPA receptors at individual GABAergic synapses in the cerebellum. J. Neurosci 2005;25:4930–4940. [PubMed: 15901774]

Sabatini BL, Svoboda K. Analysis of calcium channels in single spines using optical fluctuation analysis. Nature 2000;408:589–593. [PubMed: 11117746]

Sabatini BL, Oertner TG, Svoboda K. The life cycle of Ca^{2+} ions in dendritic spines. Neuron 2002;33:439–452. [PubMed: 11832230]

Satake S, Saitow F, Yamada J, Konishi S. Synaptic activation of AMPA receptors inhibits GABA release from cerebellar interneurons. Nat. Neurosci 2000;3:551–558. [PubMed: 10816310]

Satake S, Saitow F, Rusakov D, Konishi S. AMPA receptor-mediated presynaptic inhibition at cerebellar GABAergic synapses: a characterization of molecular mechanisms. Eur. J. Neurosci 2004;19:2464–2474. [PubMed: 15128400]

Sasaki YF, Rothe T, Premkumar LS, Das S, Cui J, Talantova MV, Wong HK, Gong X, Chan SF, Zhang D, Nakanishi N, Sucher NJ, Lipton SA. Characterization and comparison of the NR3A subunit of the NMDA receptor in recombinant systems and primary cortical neurons. J. Neurophysiol 2002;87:2052–2063. [PubMed: 11929923]

Scott R, Rusakov DA. Main determinates of presynaptic Ca^{2+} dynamics at individual mossy fiber-CA3 pyramidal cell synapses. J. Neurosci 2006;26:7071–7081. [PubMed: 16807336]

Scott R, Ruiz A, Henneberger C, Kullmann DM, Rusakov DA. Analog modulation of mossy fiber transmission is uncoupled from changes in presynaptic Ca^{2+} J. Neurosci 2008;28:7765–7773. [PubMed: 18667608]

Shin JH, Linden DL. An NMDA receptor/Nitric Oxide cascade is involved in cerebellar LTD but is not localized to the parallel fiber terminal. J. Neurophysiol 2005;94:4281–4289. [PubMed: 16120658]

Shu Y, Hasenstaub A, Duque A, Yu Y, McCormick DA. Modulation of intracortical synaptic potentials by presynaptic somatic membrane potential. Nature 2006;441:761–765. [PubMed: 16625207]

Sjostrom PJ, Turrigiano GG, Nelsonq SB. Neocrotical LTD via coincident activation of presynaptic NMDA and cannabinoid receptor. Neuron 2003;39:641–654. [PubMed: 12925278]

Soler-Llavian GJ, Sabatini BL. Synapse-specific plasticity and compartmentalized signaling in cerebellar stellate cells. Nat. Neurosci 2006;9:798–806. [PubMed: 16680164]

Sucher NJ, Akbarian S, Chi CL, Leclerc CL, Awobuluyi M, Deitcher DL, Wu MK, Yuan JP, Jones EG, Lipton SA. Developmental and regional expression pattern of a novel NMDA receptor-like subunit (NMDAR-L) in the rodent brain. J. Neurosci 1995;15:6509–6520. [PubMed: 7472413]

Tottene A, Moretti A, Pietrobon D. Functional diversity of P-type and R-type calcium channels in rat cerebellar neurons. J. Neurosci 1996;16:6353–6363. [PubMed: 8815914]

Wee KSL, Zhang Y, Khanna S, Low CM. Immunolocalization of NMDA receptor subunit NR3B in selected structures in the rat forebrain, cerebellum, and lumbar spinal cord. J. Comp. Neurol 2008;509:118–135. [PubMed: 18425811]

Yang J, Woodhall GL, Jones RSG. Tonic facilitation of glutamate release by presynaptic NR2B-containing NMDA receptors is increased in the entorhinal cortex of chronically epileptic rats. J. Neurosci 2006;26:406–410. [PubMed: 16407536]

Zucker RS, Regehr WG. Short-term synaptic plasticity. Ann. Rev. Physiol 2002;64:355–405. [PubMed: 11826273]

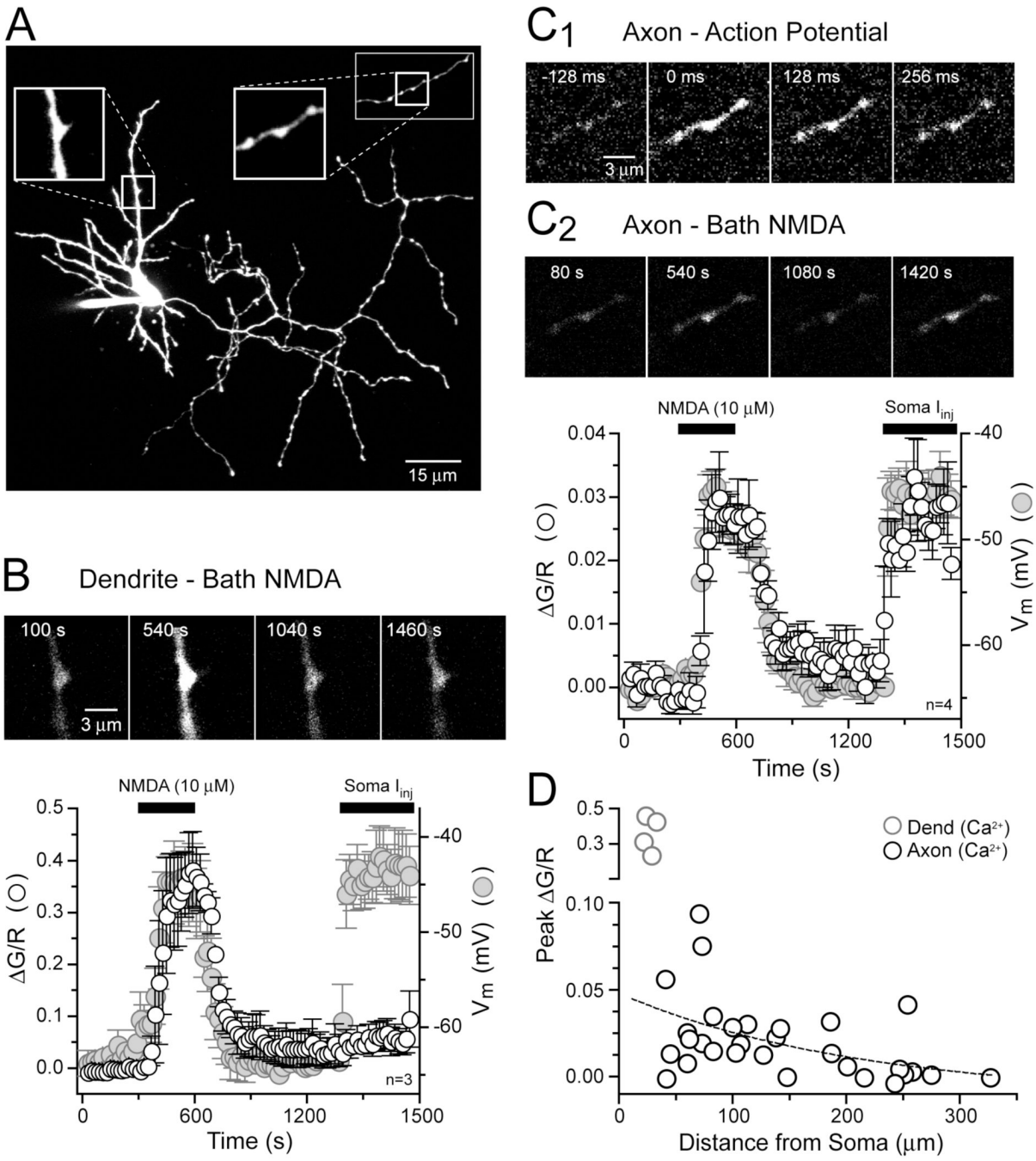

Figure 1. Bath applied NMDA evokes Ca^{2+} entry in stellate cell dendrites and axons

(**A**) Two-photon fluorescence image of a cerebellar stellate cell filled via patch pipette with 50 µM Alexa 594 and 200 µM Fluo-5F. Magnified views show a dendrite (*left boxed inset*) and an axon studded with varicosities (*right boxed inset*). The axon segment shown in the right inset is not part of the cell shown in A. (**B**) A sequence of frame scans show that application of NMDA (10 µM, 0 mM Mg^{2+}) increases Ca^{2+} in a segment of dendrite (frame 540s) while somatic depolarization (frame 1460s) resulted in very little Ca^{2+} entry. Plot shows the average Ca^{2+} increase in dendritic segments elicited by NMDA superimposed on the average somatic membrane potential. Images and voltage sweeps taken every 20 seconds. (**C_1**) Sequence of frame scans from an axon segment showing action potential-evoked Ca^{2+} entry. (**C_2**) Frame

scans from the same axon segment show Ca^{2+} entry induced by bath applied NMDA (10 μM, 0 mM Mg^{2+}) and somatic depolarization (frame 540 s and 1420 s, respectively). Plot shows the average change in Ca^{2+} recorded in axon segments and somatic membrane potential. (**D**) Dependence of axonal Ca^{2+} elevation on distance from the axon hillock (10 μM NMDA, 0 mM Mg^{2+}).

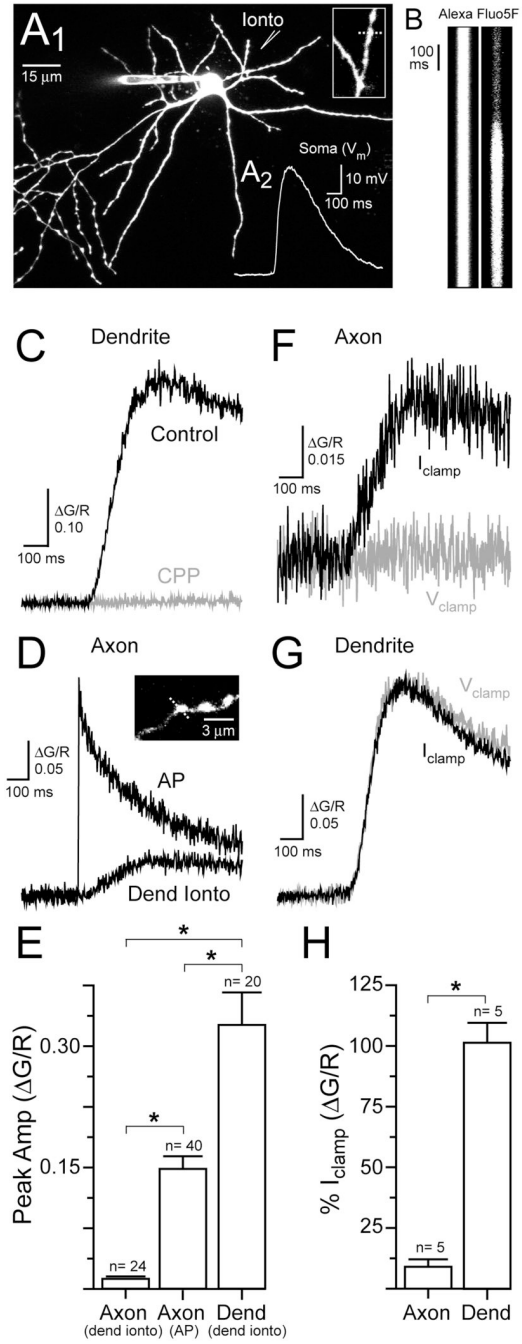

Figure 2. Dendritic NMDAR-mediated Ca^{2+} entry in axon varicosities

(**A_1**) Image of a stellate cell shows the location of the iontophoretic pipette used for dendritic *L*-aspartate application. A magnified view of the dendrite (*inset*) shows the location of the line scan (*dashed line*). (**A_2**) Dendritic iontophoresis of *L*-aspartate evoked an NMDAR-mediated depolarization (V_{rest}= −71 mV). (**B**) Line scans from the dendrite in response to *L*-aspartate iontophoretic stimulation. Iontophoretic pulse lasted 15 msec. (**C**) The iontophoresis-evoked Ca^{2+} transient recorded in the dendrite was blocked by the NMDAR antagonist (*R*)-CPP (20 µM). (**D**) Ca^{2+} transients were evoked in an axon varicosity (*inset*) by an action potential and by dendritic iontophoresis. (**E**) Average Ca^{2+} transients evoked in dendrites and axon varicosities. (**F**) Somatic voltage clamp eliminated the Ca^{2+} transient evoked in an axon

varicosity by dendritic iontophoresis. (**G**) Somatic voltage clamp did not alter the iontophoresis-evoked Ca^{2+} transient in a dendrite. (**H**) Average effect of somatic voltage clamp on Ca^{2+} transients in axons and dendrites evoked by dendritic iontophoresis.

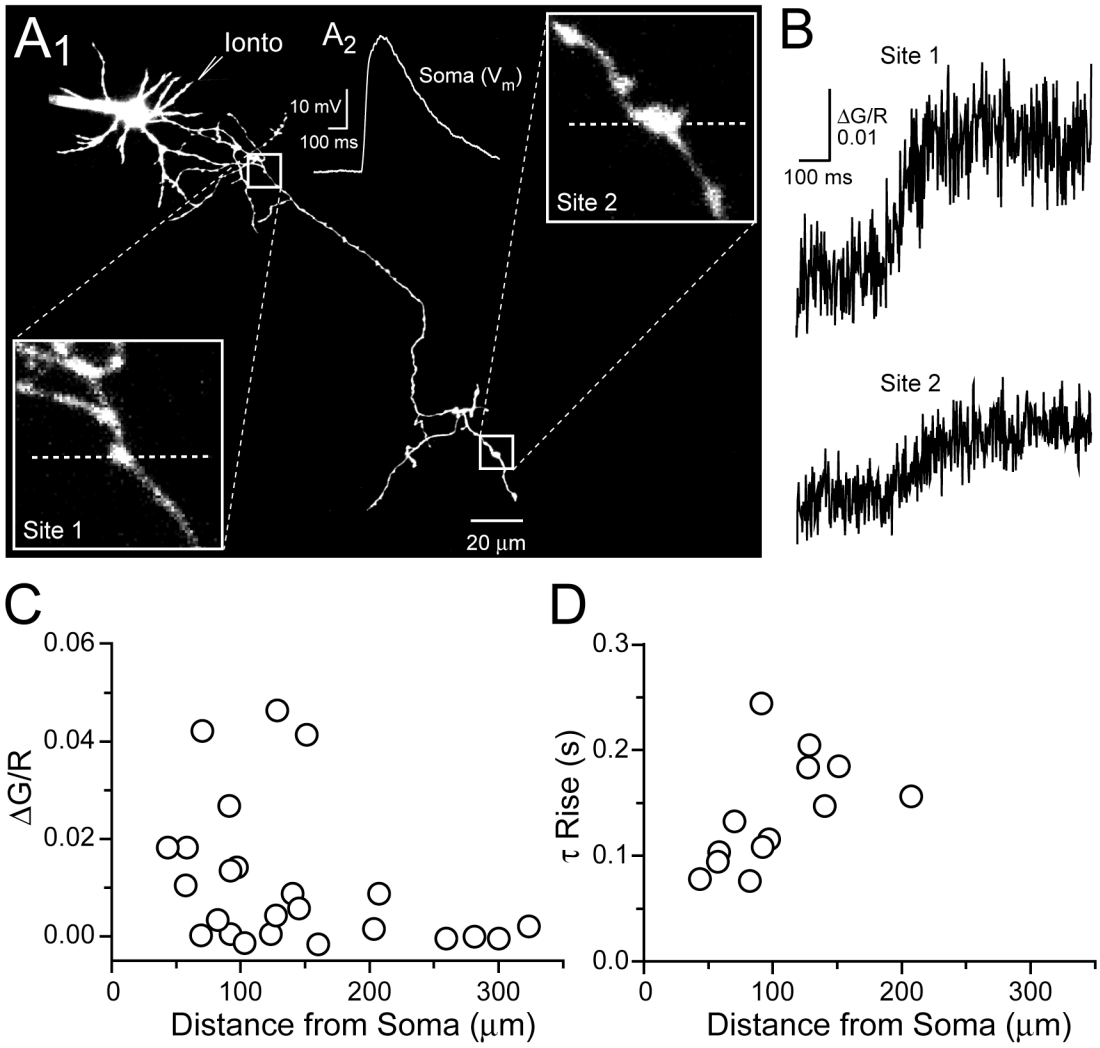

Figure 3. Distance-dependence of iontophoresis-evoked Ca^{2+} transients in axon varicosities

(**A_1**) Stellate cell image shows the axonal recording sites for Ca^{2+} measurement and the dendritic location of the iontophoretic pipette used for NMDAR stimulation. Magnified views of axonal varicosities are shown in the boxed insets with the positions of line scans (*dashed lines*). (**A_2**) An NMDAR-mediated depolarization (V_{rest}= −70 mV) resulted from dendritic iontophoresis of *L*-aspartate. (**B**) Ca^{2+} transients recorded in proximal (*site 1*) and distal (*site 2*) axon varicosities evoked by dendritic iontophoresis. (**C**) Amplitudes of Ca^{2+} transients recorded in axon varicosities versus the distance of the recording site from the axon hillock. (**D**) Single exponential fits of the rising phase of Ca^{2+} transients versus distance from the axon hillock.

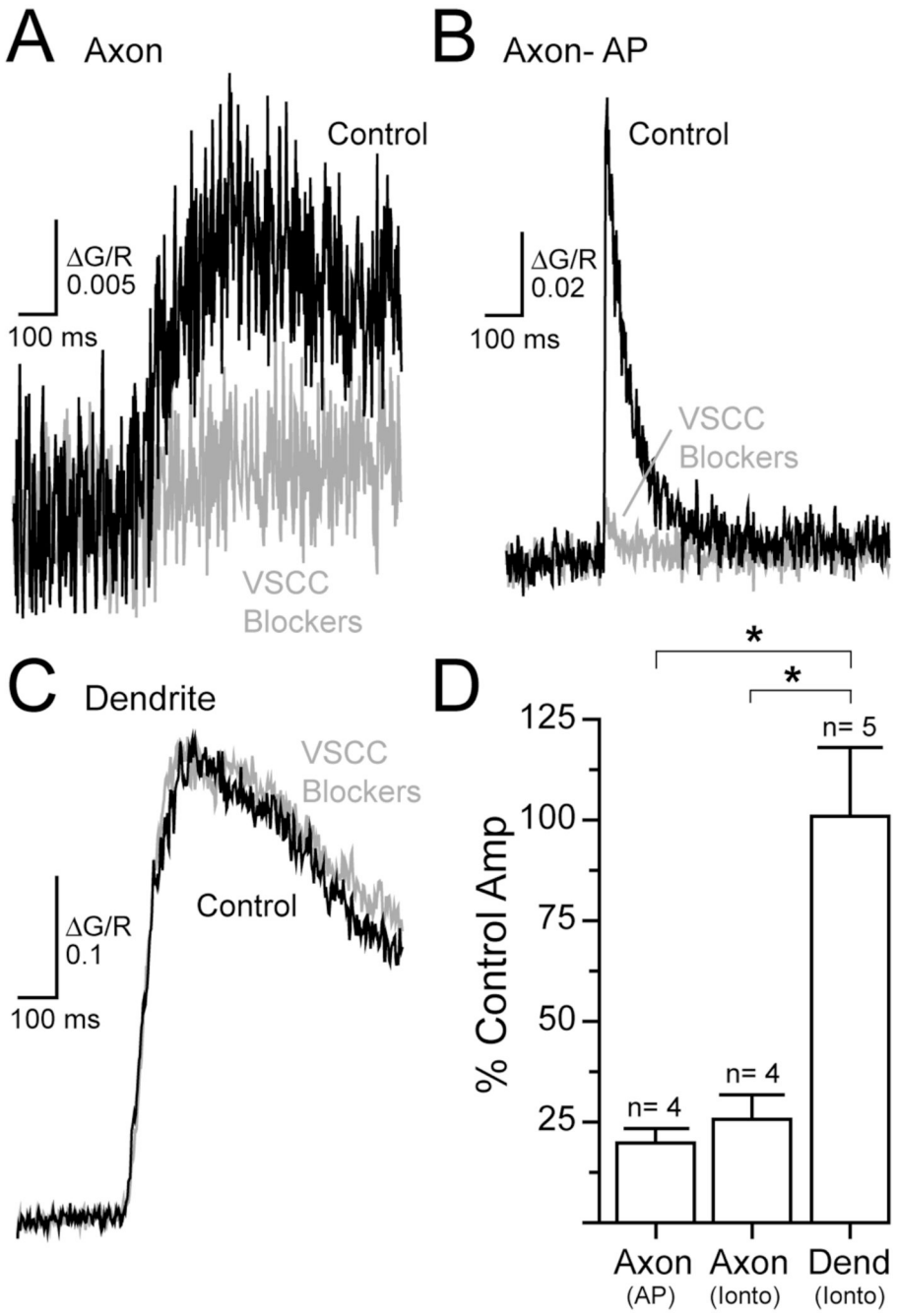

Figure 4. VSCCs mediate NMDAR-evoked Ca^{2+} entry in axon varicosities

(**A**) Dendritic iontophoresis of *L*-aspartate evoked a Ca^{2+} transient in an axon varicosity that was inhibited by a cocktail of VSCC blockers (ω-conotoxin MVIIC 1 μM, SNX 0.3 μM, ω-agatoxin IVA 0.2 μM, nimodipine 20 μM and mibefradil 10 μM) (**B**) Similarly, VSCC blockers inhibited an action potential-evoked Ca^{2+} transient in an axon varicosity.(**C**) Dendritic Ca^{2+} transient evoked by local iontophoresis was unaffected by VSCC blockers. (**D**) Inhibition of axonal and dendritic Ca^{2+} transients by VSCC antagonists.

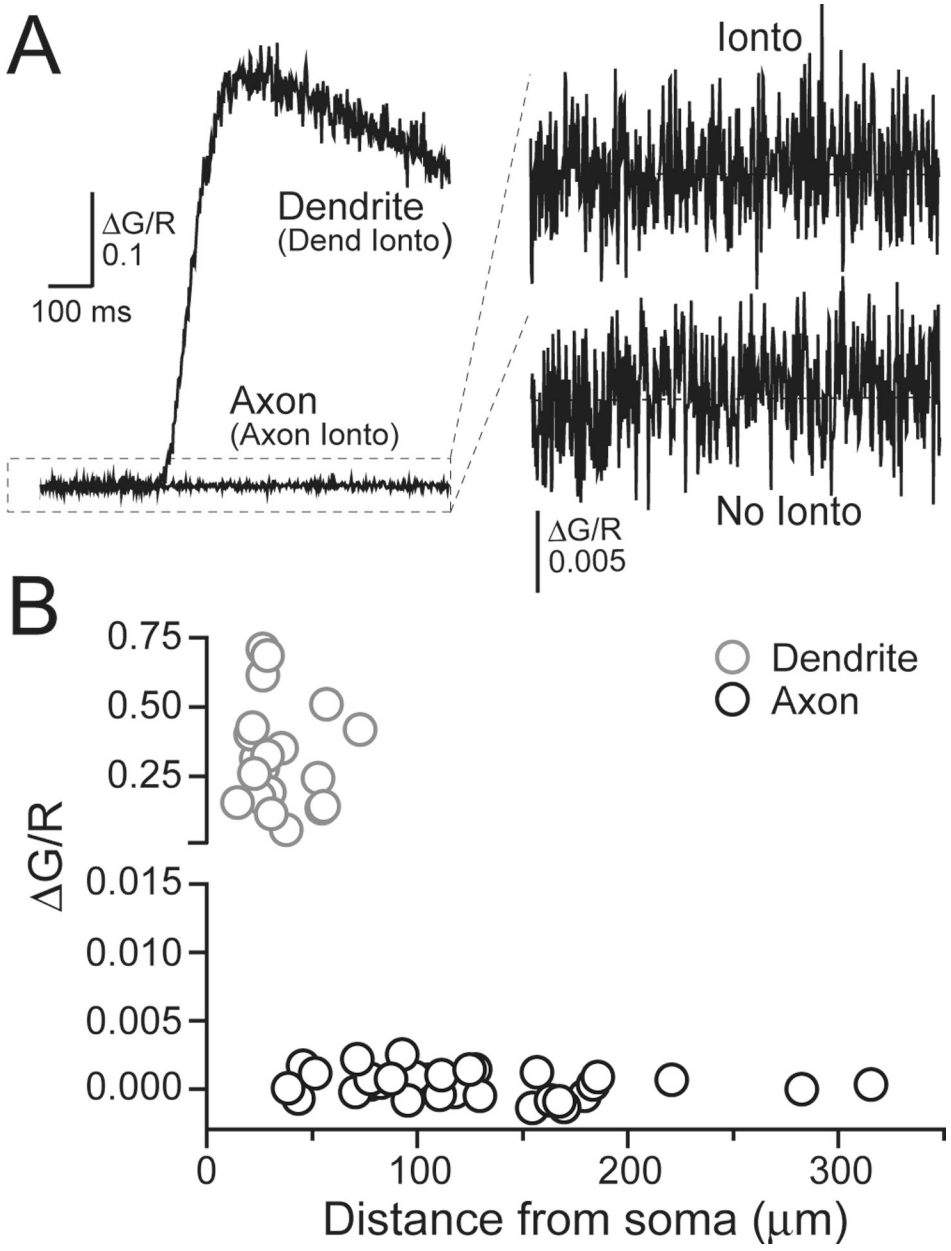

Figure 5. Axonal iontophoresis of *L*-aspartate does not evoke NMDAR-mediated Ca^{2+} transients

(**A**) Direct iontophoretic application of *L*-aspartate onto an axon varicosity failed to evoke a Ca^{2+} transient. The amplified record is shown in comparison to that without iontophoresis (each record is an average of several trials). Iontophoresis onto a dendrite of the same cell evoked a Ca^{2+} transient confirming the efficacy of *L*-aspartate application. (**B**) Peak Ca^{2+} amplitudes recorded in stellate cell processes versus distance from the axon hillock.

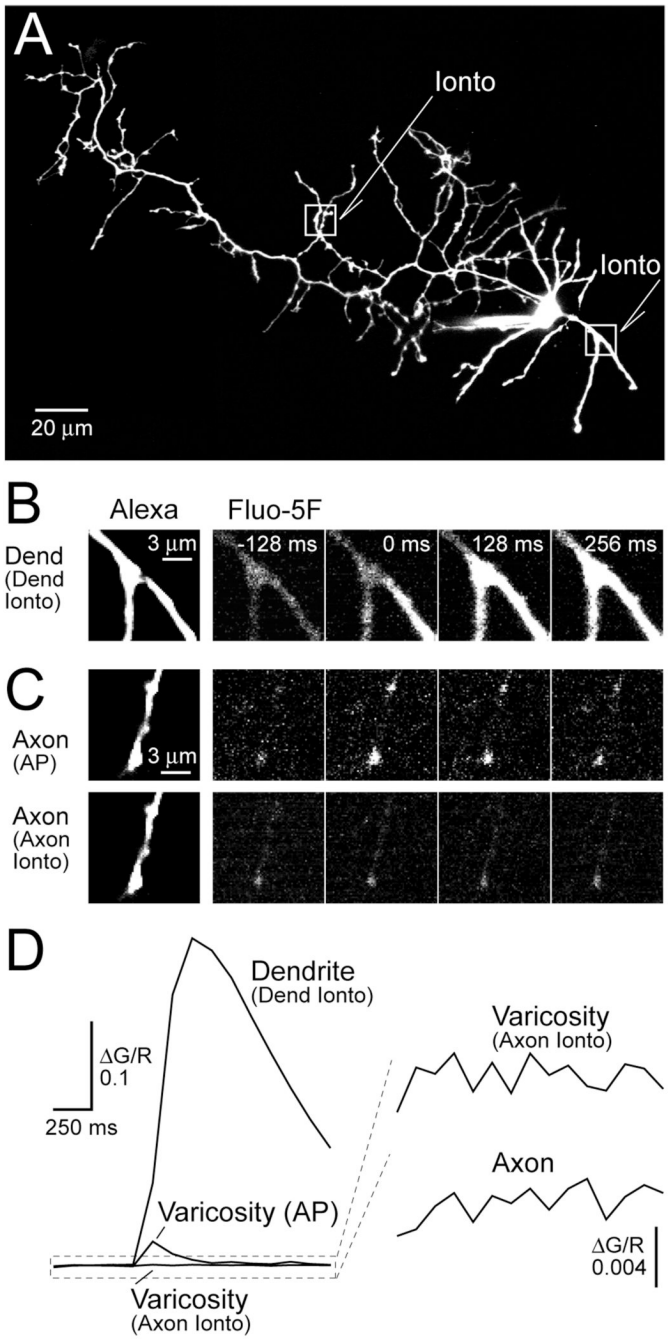

Figure 6. Stellate cell axons lack NMDARs

(**A**) Axonal (*left box*) and dendritic (*right box*) locations of *L*-aspartate iontophoresis on a stellate cell. (**B**) Frame-scan sequence shows a dendritic Ca^{2+} transient evoked by dendritic iontophoresis. (**C**) Action potential stimulation (*top*) reveals hot spots of Ca^{2+} entry in an axon segment. Frame scans taken during iontophoresis (*bottom*) onto the same axon segment. (**D**) Quantification of frame scans of dendritic (B) and axonal segments (*C- lower varicosity*) during *L*-aspartate iontophoresis.

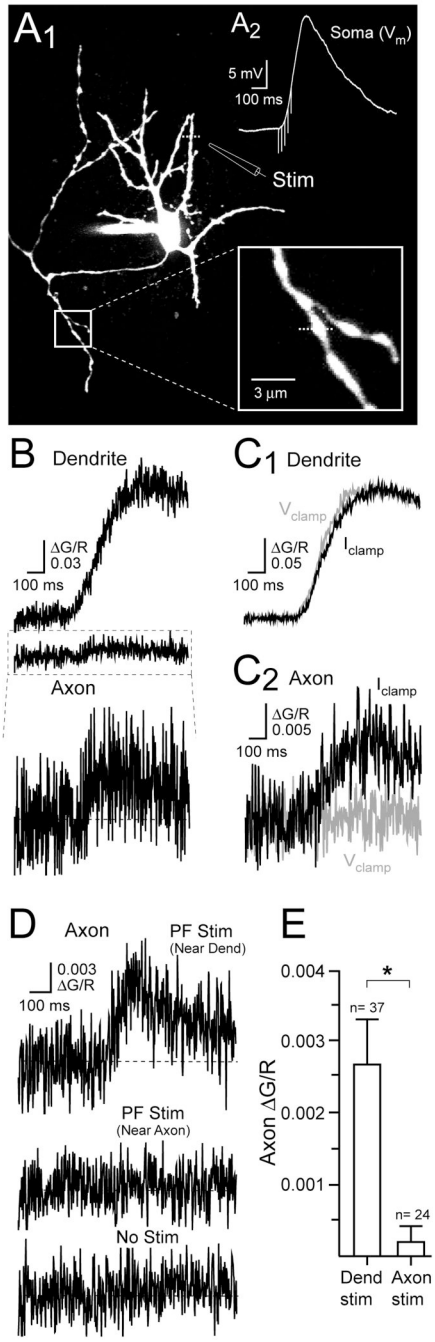

Figure 7. PF-evoked Ca^{2+} transients in axon varicosities

(**A_1**) Fluorescence image of a stellate cell shows the dendritic position of the extracellular pipette used to stimulate PFs. Magnified view of an axonal varicosity (*boxed inset*) used for Ca^{2+} imaging. (**A_2**) NMDAR-mediated EPSP evoked (V_{rest}= −70 mV) by focal stimulation of PFs (50 Hz, 80 ms). (**B**) PF stimulation evoked Ca^{2+} transients in the dendrite and axon varicosity of the cell shown in A_1. The PF-evoked axonal Ca^{2+} transient is shown (*bottom*) at higher gain. (**C_1**) Somatic voltage clamp did not alter the dendritic Ca^{2+} transient. (**C_2**) Somatic voltage clamp eliminated the Ca^{2+} transient in an axon varicosity evoked by dendritic PF stimulation. (**D**) An axonal Ca^{2+} transient evoked by dendritic PF stimulation. PF stimulation near the axon (*middle*) failed to evoked a Ca^{2+} in an axon varicosity. The axonal signal with

no stimulation (*bottom*). (**E**) Summary data show that local stimulation of PFs near axon varicosities failed to evoke a Ca^{2+} transient.